The Global Climate and Atmospheric Dynamics of Extrasolar Lava Planets

Mark Hammond

Hertford College

University of Oxford

A thesis submitted for the degree of

Doctor of Philosophy

Michaelmas Term 2019

Dedicated to whomever

Acknowledgements

Lorem ipsum dolor sit amet, consectetuer adipiscing elit. Ut purus elit, vestibulum ut, placerat ac, adipiscing vitae, felis. Curabitur dictum gravida mauris. Nam arcu libero, nonummy eget, consectetuer id, vulputate a, magna. Donec vehicula augue eu neque. Pellentesque habitant morbi tristique senectus et netus et malesuada fames ac turpis egestas. Mauris ut leo. Cras viverra metus rhoncus sem. Nulla et lectus vestibulum urna fringilla ultrices. Phasellus eu tellus sit amet tortor gravida placerat. Integer sapien est, iaculis in, pretium quis, viverra ac, nunc. Praesent eget sem vel leo ultrices bibendum. Aenean faucibus. Morbi dolor nulla, malesuada eu, pulvinar at, mollis ac, nulla. Curabitur auctor semper nulla. Donec varius orci eget risus. Duis nibh mi, congue eu, accumsan eleifend, sagittis quis, diam. Duis eget orci sit amet orci dignissim rutrum.

Abstract

This thesis aims to understand the global circulation of tidally locked lava planets, and how to interpret observations of them.

Contents

List of Figures

Chapter 1

Introduction

> *"Any finite number divided by infinity is as near to nothing as makes no odds, so the average population of all the planets in the Universe can be said to be zero. From this it follows that the population of the whole Universe is also zero, and that any people you may meet from time to time are merely the products of a deranged imagination."*
>
> — Douglas Adams, *The Restaurant at the End of the Universe*

Lava planets are rocky, very hot, and orbit so close to their host stars that they are expected to be tidally locked to them. This means that they always present the same side to the star, so have a permanent day-side and night-side. This thesis investigates the question of what these properties mean for the atmosphere of the planet, particularly its circulation and composition. Tidally locked planets are very common and observable. Lava planets are particularly observable, especially for rocky planets.

Why are tidally locked planets important? Their unusual situation could make them seem like oddities, unrelated to the majority of planets. On the contrary, Figure 1.1 shows that a large fraction of known exoplanets are expected to be tidally locked. It shows the stellar masses and semi-major axes for all exoplanets listed on the NASA Exoplanet Archive

at the time of writing, with all the planets below the line expected to be tidally locked (Pierrehumbert and Hammond, 2018).

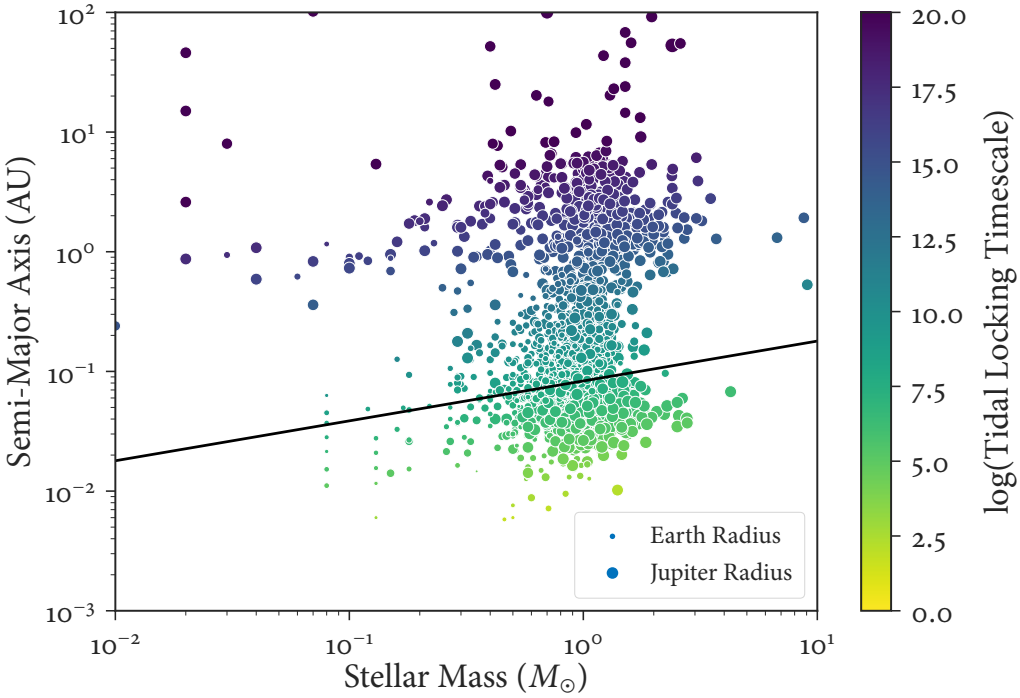

Figure 1.1: The population of known exoplanets plotted by semi-major axis and stellar mass. All the planets below the line have a timescale to reach a tidally locked state of less than 0.1 billion years, so are expected to be in this state.

These planets are also generally more easily characterised than the others, giving larger signals for spectroscopy when they transit their stars. This tendency may have created a detection bias, where close-in exoplanets are more likely to be detected so it appears that a greater fraction are tidally locked than is actually the case. Even if this is true, it does not detract from the relevance of tidally locked planets – we can only study planets we know about!

In Chapter 1, I discuss the concept of a "lava planet" and review the literature of discovery, characterisation, and modelling of such planets. I aim to introduce the scientific concepts and questions that I will address through the rest of the thesis.

In Chapter 2, I discuss the theoretical work I did to understand the global circulation of tidally locked planets in general. In the course of trying to understand simulations of tidally locked lava planets, we found that there was not a full understanding of key features of their circulation. I explain how I used a two-dimensional model to represent the atmosphere of a tidally locked planet, and demonstrated that the equatorial jet that forms affects the global circulation and temperature pattern. This was key to our work on lava planets, but was applicable to any tidally locked planet.

In Chapter 3, I introduce the model I used to simulate three-dimensional planetary atmospheres, the General Circulation Model (GCM) Exo-FMS. Developing this model formed a large part of the work of my DPhil. I discuss the structure I developed, and the physical processes represented within it. I focus on the particular challenges of simulating tidally locked lava planets, and defer many technical details to Appendix A.

In Chapter 4, I discuss my first project using these simulations to interpret observations of a lava planet.

Chapter 2

Lava Planets and 55 Cancri e

> *"One face is forever sunlit, and one forever dark, and only the planet's slow liberation gives the twilight zone a semblance of seasons."*
>
> — Stanley G. Weinbaum, *The Lotus Eaters*

Perhaps the most exciting discovery from the field of exoplanet science is that other stars host planets which are very different from those in our solar system. There are similar planets to those in the solar system – "Hot Jupiters", high-temperature Jupiter-sized gas giants in short-period orbits, or "Mini-Neptunes", which show the literal-mindedness of planetary scientists. But some exoplanets have no analogues in the solar system, and "lava planets" are some of the best examples of these.

This short chapter describes the class of "lava planets", particularly the planet 55 Cancri e, and discusses the question that this thesis aims to answers about this planet.

I will describe lava planets in general, and list the known planets in this class. I will then discuss the 55 Cancri system, and the lava planet 55 Cancri e in that system.

I will try to show that lava planets are a potentially bountiful area for scientific work, being interesting systems that have observational advantages. I will set up the question of

the atmosphere and atmospheric circulation of 55 Cancri e, and show how it relates to the broader question of the nature of the climate of tidally locked planets.

2.1 Exoplanets

Exoplanets are planets orbiting stars other than our Sun. As far as we know, there is nothing fundamental to distingush the planets in our Solar System from those elsewhere, so it is possible that this specific nomenclature may eventually disappear. I will use the word "exoplanet" when discussing specific planets or issues related to their distance, and "planet" in a more general or idealised context (such as the first sentence of this paragraph).

There is no better way to date a piece of writing on exoplanets than by announcing how many have been discovered, so I will just note that we know of several thousand and anticipate many more to come. The number of exoplanets which are favourable for detailed observations is still quite small, and we can observe atmospheric details for perhaps only a few dozen planets. In fact, while the title of this thesis suggests it looks at "lava planets", there is really only one that is currently observable – 55 Cancri e. Despite this, I hope to draw general conclusions about the circulation of many types of planet, and contribute to an understanding of tidally locked planets and lava planets for future observations.

Discovering Exoplanets

This is not a thesis on discovering exoplanets, although the methods of discovery are sometimes relevant to the characterisation that is of interest. Most exoplanets discovered to date have been found using either a "radial velocity" method or a "transit" method.

In the first method, the motion of a star around its common center of mass with a planet orbiting it is detected by measuring the Doppler-shift of emission lines of the star. The magnitude and period of this motion gives the period of the planet's orbit, and a limit on its mass.

In the second method, a planet passing across the line of sight from an observer to the star produces a dip in the light seen by the observer. A periodic dip gives the period of the planet, and the size of the dip gives its radius. So, if a planet can be measured with both methods the observer retrieves its period, mass, radius, density, semi-major axis, and equilibrium temperature.

Characterising Exoplanets

This is also not a thesis on characterising exoplanets, although I have tried to keep observations in mind throughout the simulations and theory.

The atmospheres of exoplanets can be characterised through transmission and emission spectroscopy. In transmission spectroscopy, light from the host star passes through the atmosphere of the exoplanet before it reaches the observer, and the spectrum is measured. An alternative (but equivalent) view is that the planet appears to have a different radius as it transits its star at different wavelengths – at a wavelength the atmosphere is more opaque to, the planet appears larger – so the absorption spectrum of the gases in the atmosphere can be retrieved.

In emission spectroscopy, the spectrum of the light emitted thermally by the planet and its atmosphere is measured. Hotter planets emit more light in this way, so are better

suited to this method.

2.2 Lava Planets

2.2.1 Tidally Locked Planets

A tidally locked planet, or a "synchronously rotating" planet, always presents the same face to the star it orbits, as its rotation period is the same as its orbital period. An asynchronously rotating planet like the Earth has a different rotation period (1 day) to its orbital period (1 year). Tidal forces slow down the rotation of such planets, until they become tidally locked. The time for a planet to become tidally locked is approximately:

See Chapter 3 for an investigation of the atmospheric dynamics of tidally locked planets.

Tidally locked planets include Hot Jupiters, Earth-like planets like those in the Trappist-1 system, and lava planets like 55 Cancri e, discussed next.

2.2.2 Lava Planets

"Lava Planets" are terrestrial (rocky, not gaseous) planets orbiting very close to their parent star.

2.3 55 Cancri e

55 Cancri e is a tidally locked lava planet orbiting the binary star 55 Cancri, 41 light years away in the constellation of Cancer.

The 55 Cancri system

Figure X shows the 55 Cancri system.

55 Cancri e

55 Cancri e is the closest planet to the G-star 55 Cancri A.

A Thermal Phase Curve of 55 Cancri e

A phase curve is the light measured from a planet as it orbits its star. They are particularly useful for tidally locked planets. Figure X shows a phase curve for X.

A thermal phase curve refers to the light emitted by the planet itself, rather than the light it reflects from the star it orbits. For a tidally locked planet, the thermal phase curve shows the hemisphere-averaged brightness temperature of the planet as it rotates.

Demory et al. (2016) measured a thermal phase curve of the planet 55 Cancri e.

55 Cancri e is currently the most easily observable terrestrial tidally locked planet. Its composition, atmosphere, and circulation provide tests of theories of planet formation and atmospheric dynamics. In this thesis, I will use it as a case study for the atmospheric dynamics of tidally locked planets.

Chapter 3

Wave-Mean Flow Interactions in a Linear Theory of Tidally Locked Atmospheres

"One might as well approximate the derivatives well instead of badly"
— John P. Boyd, *Chebyshev and Fourier Spectral Methods*

Tidally locked planetary atmospheres have such a different spatial energy input to planets like the Earth that it is not obvious that conventional Earth-like atmospheric dynamics should be able to describe them. However, the planetary-scale day-night forcing difference makes the global circulation highly susceptible to a simple shallow-water model, compared to the higher order effects controlling the Earth's atmosphere.

This chapter discusses my work using a single-layer linear shallow-water model to investigate the global circulation of tidally locked planets. It follows directly from the work of XX and XX.

After introducing the linear shallow-water model and the work of Matsuno, Gill, Showman, and Tsai, I will show how I linearised the model about a zonally uniform jet $\bar{U}(y)$ with latitudinal shear, as well as its associated geostrophic height perturbation $\bar{H}(y)$

A formula:

$$\underbrace{\frac{\sin^2\vartheta}{\Theta_{lm}(\vartheta)}\left(\frac{\partial^2}{\partial\vartheta^2}+\frac{\cos\vartheta}{\sin\vartheta}\frac{\partial}{\partial\vartheta}\right)\Theta_{lm}(\vartheta)+\sin^2(\vartheta)(l(l+1))}_{m^2}=\underbrace{-\frac{1}{\Phi_m(\varphi)}\frac{\partial^2}{\partial\varphi^2}\Phi_m(\varphi)}_{m^2}$$

and another one:

$$P_l(x)\equiv\frac{1}{2^l}\sum_{k=0}^{\lfloor l/2\rfloor}(-1)^k\frac{(2l-2k)!}{k!(l-k)!(l-2k)!}x^{l-2k}$$

I will show that linearising the jet about the shear flow and its height perurbation makes the forced linear response match nonlinear GCM simulations much more closely. The new model reveals scaling relations between the planetary parameters such as forcing strength, and the observable quantities such as the eastward hot-spot shift.

3.1 The Shallow-Water Equations

A Linear, Single-Layer Beta-Plane System

We used the linear shallow-water equations on a one-layer equatorial beta-plane to model the atmosphere of a tidally locked planet. These equations describe the motion of a single layer of fluid of constant density where the horizontal scale of its flow is much greater than the depth of the fluid. The linear form of these equations describe small perturbations to this layer (Vallis, 2006). We model the atmosphere of a tidally locked planet with a similar shallow-water model to Showman and Polvani (2011). The model corresponds to an active upper layer following the single-layer shallow water equations, above a quiescent layer which can transport mass and momentum to and from the upper layer. The forcing due to stellar heating is represented by Q, a relaxation to the radiative equilibrium height field.

In this section, we derive the wave response to stationary forcing on the beta-plane (Matsuno, 1966). The beta-plane system approximates the Coriolis parameter as linear, which is only accurate at low latitudes but leads to more intuitive and useful solutions than the full spherical geometry. We solve the equations in a spherical geometry in Section **??**, and show that the beta-plane approximation leads to very similar solutions, as in other studies of the atmospheres of tidally locked planets (Showman and Polvani, 2011) (Heng and Workman, 2014).

All the quantities are linearized as the sum of a zonally mean background value $F(y)$ and a perturbation with the form $f(y)e^{i(k_x x-\omega t)}$ (unlike Matsuno (1966), who uses the less conventional form $f(y)e^{i(k_x x+\omega t)}$). Throughout this paper, we will use capital letters for mean zonal quantities such as $\bar{U}$ and $\bar{H}$, and lower-case letters for perturbations to this background, such as u and h (unless otherwise specified, such as the forcing Q). The shallow-water equations for these perturbations with zero background flow are:

$$\begin{aligned} \frac{\partial u}{\partial t} - \beta y v + \frac{\partial h}{\partial x} &= 0 \\ \frac{\partial v}{\partial t} + \beta y u + \frac{\partial h}{\partial y} &= 0 \\ \frac{\partial h}{\partial t} + c^2\left(\frac{\partial u}{\partial x} + \frac{\partial v}{\partial y}\right) &= 0 \end{aligned} \tag{3.1}$$

where h is the height, $c = \sqrt{gH}$ is the gravity wave speed (Matsuno, 1966), and there is no friction or damping. Non-dimensionalizing with time scale $\sqrt{1/c\beta}$ and length scale $\sqrt{c/\beta}$ (the equatorial Rossby radius of deformation L_R), and assuming all quantities have the form $f(y)e^{i(kx-\omega t)}$, the free equations are:

$$\begin{aligned} -i\omega u - yv + ik_x h &= 0 \\ -i\omega v + yu + \frac{\partial h}{\partial y} &= 0 \\ -i\omega h + iku + \frac{\partial v}{\partial y} &= 0 \end{aligned} \tag{3.2}$$

Jet Acceleration

Wave Interactions with Uniform Flow

3.2 Zonal Acceleration

Chapter X showed that the global circulation and temperature distribution of an atmosphere on a tidally locked planet depends greatly on the zonal jets present on the planet.

Acceleration in a Matsuno-Gill Model

The zonally averaged zonal momentum equation is:

$$\frac{\partial \overline{u}}{\partial t} = \underbrace{\overline{v}^* \left[f - \frac{\partial \overline{u}}{\partial y} \right]}_{I} \underbrace{- \frac{1}{\overline{h}} \frac{\partial}{\partial y} \left[\overline{(hv)' u'} \right]}_{II} + \underbrace{\left[\frac{1}{\overline{h}} \overline{u' Q'} + \overline{R_u}^* \right]}_{III} \underbrace{- \frac{\overline{u}^*}{\tau_{\text{drag}}}}_{IV} - \frac{1}{\overline{h}} \frac{\partial \left(\overline{h' u'} \right)}{\partial t} \tag{3.3}$$

In the Matsuno-Gill model, this gives zero acceleration at the equator without R.

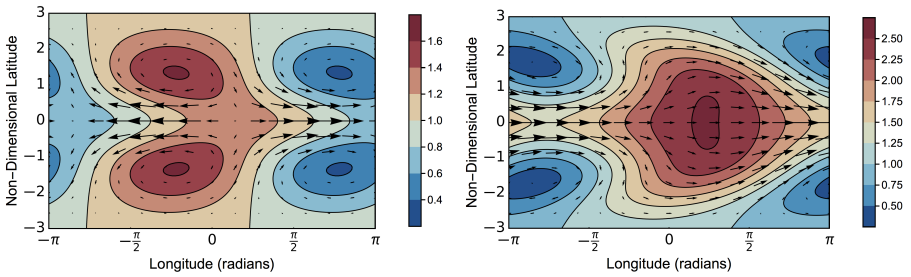

(a) Zero Flow. (b) Shear Flow.

Figure 3.1: Zero Flow and Shear Flow.

Vertical Momentum Transport

Horizontal Momentum Transport from Stationary Waves

3.3 Wave Interactions with Shear Flow

Shear Flow on the Beta-Plane

Shear Flow on a Sphere

3.4 Scaling Relations

1D Scaling Relations

2D Scaling Relations

Chapter 4

Non-Linear Tests of a Linear Theory of Tidally Locked Atmospheres

"One might as well approximate the derivatives well instead of badly"
— John P. Boyd, *Chebyshev and Fourier Spectral Methods*

In this chapter, I test the mechanism for the circulation of tidally locked planetary atmospheres predicted in the previous chapter. I use a single-layer non-linear shallow-water model, and a 3D General Circulation Model (GCM) to simulate the atmosphere, and compare the results to the linear theory.

The linear theory simplified the system of a tidally locked planetary atmosphere greatly, and these tests will investigate whether these assumptions were accurate, and test how well the theory predicts the equilibrium circulation.

I will introduce the models used, and show basic tests of whether the mechanism predicted by the linear model is actually at work. I will test the spin-up and equilibrium states of the non-linear models, and compare the results to the scaling relations predicted by the linear model.

This chapter will show that the linear model is a good approximation to the results of the non-linear simulations. The wave-mean flow interaction in the linear theory also applies to the non-linear simulations, suggesting that this is at work on real tidally locked planetary atmospheres as well.

4.1 Non-Linear Tests of Linear Shallow-Water Theory

The linear model in Chapter 3 made X main simplifications:

1. The perturbations to the atmosphere are small enough to be approximately linear.
2. The atmospheric response is (on average) stationary, and any transient behaviour does not affect the mean circulation.
3. The atmosphere and the variations in it are small enough in the vertical to be approximated by a shallow model.
4. The day-night forcing is approximated by a relaxation to a constant radiative equilibrium height field.

This section discusses tests of the single-layer linear theory in Chapter 3 using a single-layer non-linear model, which removes the first two assumptions.

Non-Linear Shallow-Water Model

I used the Geophysical Fluid Dynamics Laboratory Flexible Modelling System (FMS) Spectral Dynamical Core (GFDL-SDC) for non-linear shallow-water simulations. Appendix B describes the model setup.

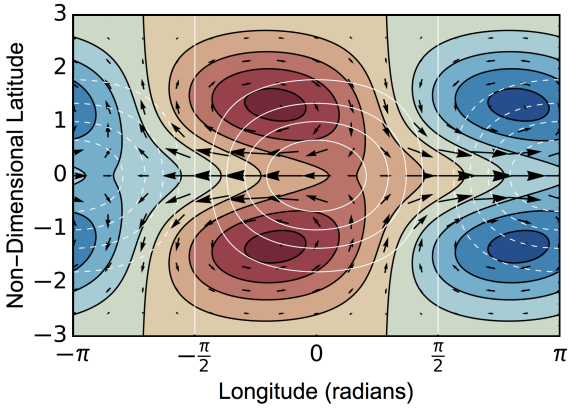

Figure 4.1: The linear response.

Testing Linearity

The linear model in Chapter 3 is based on a forced linear shallow-water system as discussed in Matsuno (1966). Figure 4.1 shows the response to a forcing $Q(x, y) = \sin(x)e^{-y^2/2}$ in this linear system.

The linear model assumes that the perturbations in the shallow-water system (representing perturbations in a real three-dimensional atmosphere) are small enough that the linear terms dominate the shallow-water equations. I ran simulations in the non-linear shallow-water model to test whether they matched the linear model at appropriate forcing strength.

The non-linear shallow-water equations are:

The linear solution in spherical coordinates in Figure X in Chapter X has $\alpha_{rad} = \alpha_{dyn} = 0.2$, $G = 1$ and $\Delta h/H = 0.5$. To match this in the non-linear model, I set $\alpha_{rad} = \alpha_{dyn} = 0.2$, $\Delta h = 5$ km, and $H = 10$ km. To set $G = 1$, I set $R = R_{Earth}$ and $g = 10$, then tuned the rotation rate to $\Omega = 4.964 \times 10^{-5} = 0.6807\Omega_{Earth}$.

Figure 4.2 shows the equilibrated height and velocity fields for the non-linear model with these parameters, and zero imposed background flow. The non-linear model matches the linear model in Figure X well, with a similar pattern and perturbation size. There is a small day-night asymmetry in the non-linear mode which is not present in the linear model.

The plots in Figure 4.3 show the non-linear response with a smaller height perturbation Δh = 1 km, and a larger height perturbation Δh = 20 km. Figure 4.3a with the smaller perturbation has a smaller day-night asymmetry than Figure X.b, which is expected as the smaller perturbation should produce a more linear response. Figure 4.3b with the larger perturbation has a larger day-night asymmetry than Figure 4.2, which is expected as the larger perturbation should produce a less linear response. The pattern is also more different from the linear pattern, showing that the linear approximation is less appropriate at the higher forcing amplitude.

This is all as expected, and shows that the forcing amplitudes used in the linear solutions in Chapter X ($\Delta h/(H\tau_{rad} \sim 0.1$) and the GCM simulations in Chapter X ($\Delta T/(T \sim 0.1$) are in a regime that is well represented by the linear approximation.

It is possible that the background flow that is imposed in the linear solutions and emerges in the GCM simulations affects the size of the perturbations and moves the system out of the linear regime. I ran the same non-linear shallow-water simulations as Figure X, but imposed the same jet as in the linear solutions to test if the linear and non-linear solutions still matched.

The simulations had the same parameters as in Figure 4.2. The linear model in spherical geometry in Chapter X has a jet with a non-dimensional velocity of

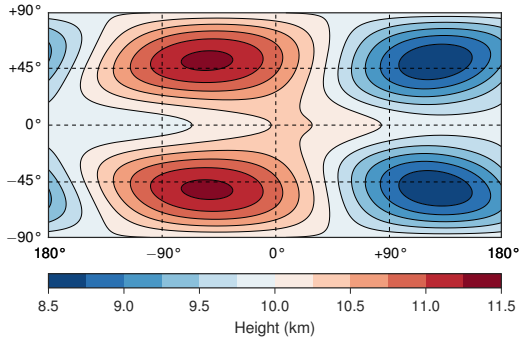

Figure 4.2: 5e3.

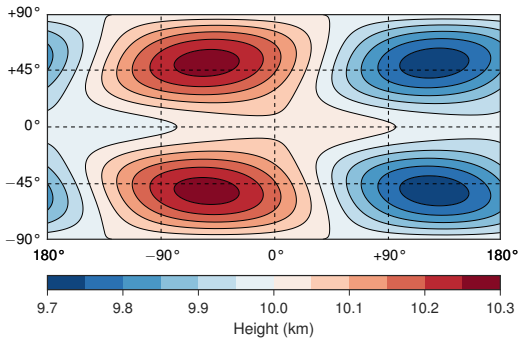

(a) 1e3.

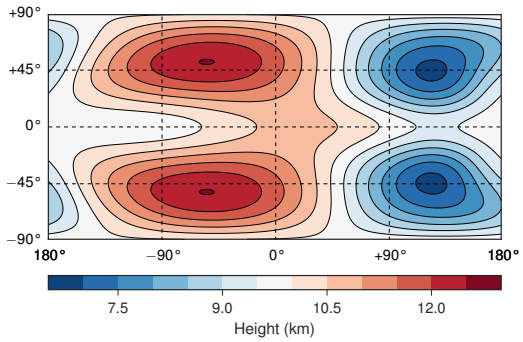

(b) 1e4.

Figure 4.3: Nonlinear.

$0.5 \cos\phi \exp(-(\phi/\phi_0)^2)$, with a jet width $\phi_0 = \pi/3$. The non-linear system in Figure 4.2 has a velocity scale of $R\Omega$, so I relaxed the non-linear simulations on a timescale $\tau_{dyn} = 1/\alpha_{dyn}$ to a background flow profile $R\Omega \cos\phi \exp(-(\phi/\phi_0)^2)$. Figure 4.4 shows the equilibrated response.

The non-linear response has much less shift at higher latitudes, and a much narrower zonal height field. The zonal flow profile is much narrower than the imposed profile. Figure X shows that subtracting the background flow that is imposed leaves a large retrograde

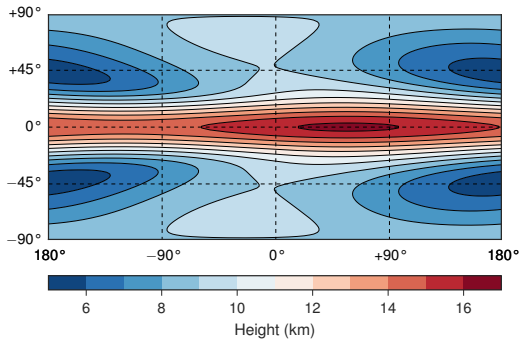

Figure 4.4: Matsuno jet control.

flow in the midlatitudes, as forms in the non-linear Matsuno case. Figure X shows the response and the mean zonal velocity of the case which is not relaxed towards a background flow (the same test as Figure 4.2). This case has westward flow in the midlatitudes, as predicted by Figure X in Chapter X. This mechanism causes the reduced eastward flow in the midlatitudes in the case with a jet in Figure X.

This is responsible for the main difference between the linear and non-linear model. In fact, the acceleration calculated in the linear model does predict this westward midlatitude flow, but it was ignored in Chapter X to match the GCM results.

This highlights a difference between the GCM and the shallow-water models. The shallow-water models always predict a westward acceleration in the mid-latitudes, but this is rarely seen in the GCM. In Chapter X I suggest that eastward acceleration from Rossby wave breaking is responsible for the midlatitude eastward flow in the GCM.

These simulations have shown that the linear model is an appropriate approximation for the atmosphere of a tidally locked planet, but that it does not correctly predict the acceleration away from the equator.

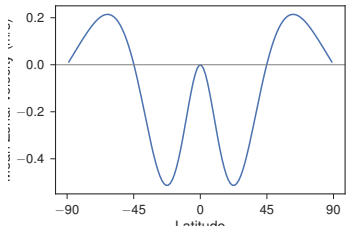

(a) m-control$_mean - u$.

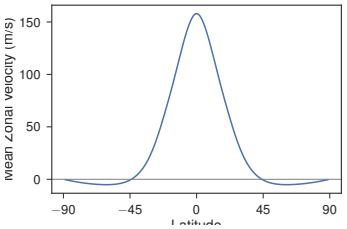

(b) m-jet-control$_mean - u$.

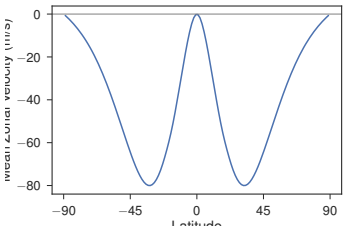

(c) m-jet-control$_mean - u - minus - U$.

Figure 4.5: Nonlinear.

Testing Equilibrium State

Chapter X discusses the jet acceleration.

The time-stepped model reaches an equilibrium state after about X days. The transient response from the impulse generated by turning on the forcing dissipates, and a steady state is reached.

Show wave components, hot-spot, and wind directions.

Figure X shows the equilibrium state for the model with forcing X and rotation rate X. Figure X shows the eddy state, showing how the waves have shifted.

Testing Jet Spin-up

I ran tests to show how the atmosphere reaches this state.

Figure X shows the eddy state over time of the previous test.

Figure X shows the Rossby and Kelvin components over time of the previous test.

Spin-up of height field, eddy height field, and Rossby and Kelvin components.

Scaling Relation Tests

Test effect of rotation rate, forcing, jet speed.

Figure X shows the equilibrium state for the model with the same forcing X and different rotation rates X.

Figure X shows the equilibrium state for the model with different forcing X.

Figure X shows the equilibrium state for the model with different jet speed X.

4.2 GCM Tests of Shallow-Water Theory

I used the GCM Exo-FMS, based on the Geophysical Fluid Dynamics Laboratory Flexible Modelling System (GFDL-FMS). Chapter 6 and Appendix A describe this model.

Testing Equilibrium State

Show wave components, hot-spot, and wind directions.

Testing Jet Spin-up

Spin-up of height field, eddy height field, and Rossby and Kelvin components.

Scaling Relation Tests

Test effect of rotation rate, forcing, jet speed.

Chapter 5

Equilibrium Circulation States on Tidally Locked Planets

"Very strange," he said. "A permanent anticyclone, and inside a huge, calm land that never sees a storm and never has a drop of rain."

"Good place for a holiday then!"

— Terry Pratchett, *The Last Continent*

Tidally locked planetary atmospheres

5.1 Equatorial Acceleration

Chapter X showed that the global circulation and temperature distribution of an atmosphere on a tidally locked planet depends greatly on the zonal jets present on the planet.

Acceleration in a Matsuno-Gill Model

The zonally averaged zonal momentum equation is:

$$\frac{\partial \overline{u}}{\partial t} = \underbrace{\overline{v}^* \left[f - \frac{\partial \overline{u}}{\partial y} \right]}_{I} \underbrace{- \frac{1}{\overline{h}} \frac{\partial}{\partial y} \left[\overline{(hv)' u'} \right]}_{II} + \underbrace{\left[\frac{1}{\overline{h}} \overline{u' Q'} + \overline{R_u}^* \right]}_{III} \underbrace{- \frac{\overline{u}^*}{\tau_{\text{drag}}}}_{IV} - \frac{1}{\overline{h}} \frac{\partial \left(\overline{h' u'} \right)}{\partial t} \tag{5.1}$$

Vertical Momentum Transport

Horizontal Momentum Transport from Stationary Waves

Horizontal Momentum Transport from Transient Waves

5.2 Midlatitude Acceleration

Chapter X showed that the global circulation and temperature distribution of an atmosphere on a tidally locked planet depends greatly on the zonal jets present on the planet.

Acceleration from Rossby Wave Breaking

Scaling

GCM Simulations

Figure X shows a suite of tests (P+H2019) showing how the number of jets varies with rotation rate and temperature.

Figure X shows the spin-up of a very rapidly rotating case.

5.3 Initial Conditions

Starting from Rest

Initially Retrograde Flow

Initially Strong Prograde Flow

5.4 Instabilities as deviations from equilibrium

Linear Model Instability Analysis

The linear model predicts instabilities.

Instabilities in GCM

Instabilities appear in the GCM

5.5 Jet Scaling Relations

Equatorial versus Midlatitude Jets

Chapter 6

Simulating Tidally Locked Exoplanets with Exo-FMS

> *"One face is forever sunlit, and one forever dark, and only the planet's slow liberation gives the twilight zone a semblance of seasons."*
>
> — Stanley G. Weinbaum, *The Lotus Eaters*

Three-dimensional simulations are an important tool for understanding atmospheric dynamics and climate.

A General Circulation Model (GCM)

This chapter describes my work on the GCM Exo-FMS, and discusses the specific needs and issues of the atmospheres that I simulated with it.

I will discuss the dynamical core and grid of the model

This chapter does not include much scientific investigation, but I will try to show that an exoplanet GCM is not a fanciful attempt to recreate an unknowable planet, but can be used carefully alongside basic theories and real observations to understand processes that are only apparent in a full 3D representation of the planetary atmosphere. I will also argue

that XX.

6.1 Model Structure

GFDL-FMS

Exo-FMS is based on the cubed-sphere dynamical core of the GFDL FMS.

Github Repository

It was very important that Exo-FMS should be openly available. I manage its Github repository and wiki.

ExoFMS Interface

Exo-FMS is meant to make the fewest modifications to the original FMS structure and cubed-sphere dynamical core as possible. To this end, I wrote a single interface to couple the dynamical core to our physics modules (radiative transfer, convection etc.).

6.2 Dynamics

6.3 Radiative Transfer

6.4 Cloud Microphysics

Chapter 7

Linking the Climate and Thermal Phase Curve of 55 Cancri e

"One face is forever sunlit, and one forever dark, and only the planet's slow liberation gives the twilight zone a semblance of seasons."

— Stanley G. Weinbaum, *The Lotus Eaters*

Now that I have introduced lava planets and 55 Cancri e in Chapter X, laid out a theory of their circulation in Chapters X and X, and discussed the numerical model I used to simulate them in Chapter X, I can move to the central question of this thesis. Namely, how to interpret the thermal emission phase curve of a tidally locked lava planet? The remaining chapters of my thesis will investigate this in increasing detail.

The first phase curve of a Super-Earth was measured by Demory et al. (2016) using Spitzer observations of 55 Cancri e, following the measurement of transits in the visible (Winn et al., 2011) and infrared (Demory et al., 2011). This presented the first observation directly linked to the global circulation of a terrestrial planet outside our solar system. It provides an opportunity to test the theories and simulations of the atmospheric circulation

of a tidally locked planet that have been shown previously in this thesis.

The thermal phase curve of 55 Cnc e presents the possibility of testing this picture of lava planets, and in particular to determine whether the phase curve demands the presence of a thick noncondensible background atmosphere. In this paper, we use a general circulation model (GCM) to model a range of hypothetical climates for 55 Cnc e and reconstruct their thermal phase curve, in order to test whether the observed phase curve is inconsistent with the presence of a thick atmosphere. We explore which atmospheric compositions are compatible with the phase curve. The results we have obtained for 55 Cnc e will carry over readily to the interpretation of other lava planet phase curves when they become available. The general utility of thermal phase curves in determining characteristics of exoplanets and their atmospheres has been discussed in Selsis et al. (2011) and Maurin et al. (2012).

The analysis in this paper builds on the results of Cowan Agol (2011), Menou (2012), and Komacek Showman (2016), who explored the effect of parameters such as the mean molecular weight on the thermal phase curve of Hot Jupiters via the radiative and advective timescales. Koll Abbot (2015) modelled the relation between atmospheric properties and broadband thermal phase curve for terrestrial planets in a regime (expected to be appropriate to most tidally locked planets) with a significant phase curve amplitude, but very little hot-spot offset. We have identified a regime which can support both a notable amplitude and offset.

Section 2 describes our model and explains the physical processes which it includes. Section 3 lays out the current theory of global circulation on tidally locked planets, where we discuss the key nondimensional parameters and situate 55 Cnc e in the space of circulation regimes. We describe the results from our experiments in Section 4, focusing on

their temperature distributions and simulated phase curves in comparison to the results of Demory et al. (2016b). Further interpretation of the results is provide in Section 5 and our principal findings are summarized in Section 6.

Our best-fit clear-sky atmosphere has a surface pressure of 5 bar and a mean molecular weight of 4.6 gmol1 . This molecular weight would support the hypothesis of an H2-rich atmosphere; however, it is the observed hot-spot phase shift which favours low molecular weight, underscoring the importance of accurate measurements of this quantity for future observations of 55 Cnc e and other lava planets. A diagnostic estimate of cloud effects indicates that Na clouds would not form in such an atmosphere, but that SiO clouds could form on the night-side and bring the modeled night-side brightness temperature more in line with observations. Our results on the vertical structure of the temperature pattern underscore the importance of future measurements of spectrally resolved phase curves for 55 Cnc e and other lava planets, which would provide an important window into atmospheric composition and dynamics.

In the next chapter, I will show how we coupled a more realistic radiative transfer scheme and a dynamic cloud model to Exo-FMS, in order to test the questions raised by this chapter.

7.1 Observations of 55 Cancri e

55 Cancri e

The first phase curve of a Super-Earth was measured by Demory et al. (2016b) using Spitzer observations of 55 Cancri e, following the measurement of transits in the visible

(Winn et al. 2011) and infrared (Demory et al. 2011). 55 Cnc e is a Super-Earth discovered by McArthur et al. (2004) with mass 8.63 M and radius 2.00 R in a close, tidally locked orbit with period 0.737 days.

Thermal Phase Curve

The thermal phase curve has a large amplitude and an offset between its secondary eclipse and its phase maximum. Demory et al. (2016b) used the curve to reconstruct a temperature map with a maximum hemisphere-averaged 4.5µm brightness temperature of (2700 ± 270) K, day-night contrast of (1300 ± 670) K, and a hot-spot shifted eastwards by (41 ± 12)■ .

Possible Atmosphere

55 Cnc e is a member of a class of planets known as "lava planets" which are in such close orbits that they are likely to be tide-locked and have a permanent dayside magma ocean. It has been argued that the atmospheres of such planets could consist of thin mineralvapour atmospheres outgassed from the magma ocean (L´eger et al. 2011) (Castan Menou 2011). Such thin atmospheres, consisting of a few millibar or less surface pressure, cannot transport much heat apart from possible lateral heat redistribution within the magma ocean, so would yield a phase curve very similar to that of an airless rocky planet with a very cold night-side such as discussed by Maurin et al. (2012).

The transit depth spectra reported in Tsiaras et al. (2016) require a thick H2-rich atmosphere. However, Lammer et al. (2013) calculated that an H2 atmosphere on 55 Cnc

e would have a hydrodynamic escape rate of up to 2.8 × 109 gs1 . This implies that a 10 bar atmosphere would be lost in less than one million years, making it implausible that an H2-rich atmosphere could be maintained on this planet. However, the study of exoplanets has yielded up many objects that according to previous conceptions should not exist, so in this paper we will take the idea of an H2-rich atmosphere seriously, and ask what features of the phase curve measured by Demory et al. (2016b) are compatible with, or demand, a low molecular weight atmosphere. In order to focus on dynamical behavior in this initial study, we make a number of simplifying assumptions regarding the radiative behavior of the atmosphere. First, we assume the atmosphere to be transparent to incoming stellar radiation, so that all of the shortwave radiation is absorbed at the ground, leading to a deep day-side convective layer. This assumption is based on estimates of the shortwave opacity of likely cloud-free atmospheres of up to 10 bars. The addition of a small amount of shortwave opacity would not change our results much, so long as atmospheric absorption occurs near enough the surface to drive a convective troposphere. Very thick shortwave-opaque atmospheres could instead have a deep radiative-equilibrium layer with a thin dynamically active layer near the top; we shall not consider such atmospheres in the present paper. In the infrared, the atmosphere is assumed to act as a grey gas with specified optical thickness and opacity . This is not inconsistent with the assumption of an atmosphere largely transparent to incoming stellar radiation, because 55 Cancri is a G star, with a relatively low proportion of its output in the near-IR. The use of gray gas radiation for climate calculations is not a serious source of inaccuracy as the circulation is primarily affected by the radiation scheme via the surface temperature relative to the radiating temperature of the planet. The optical thickness can be tuned to match the temperature that

would be yielded by an assumed real-gas atmosphere, so in this paper we use primarily as a way to control surface temperature. Non-grey radiative effects are taken into account when we interpret the results in terms of the corresponding Spitzer 4.5μm phase curve, in that we consider the emission from a range of different atmospheric levels and not just the grey radiating level. This allows for the possibility that the atmospheric composition may support an infrared window region near 4.5μm, allowing radiation from deeper in the atmosphere, or a source of anomalous opacity (e.g. clouds) there, forcing the radiating level to be higher in the atmosphere. The surface pressure determines the atmospheric mass via the hydrostatic relation. For a given surface pressure and , atmospheric composition affects the climate through mean molecular weight and specific heat. However, molar specific heat is only weakly dependent Climate of 55 Cancri e 3 on composition, because it is primarily determined by the number of active degrees of freedom. For example, at 2000K the molar specific heats of CO, N2 and H2 vary by no more than 3.435.5 Jmol1K1 , with similar results for other common diatomic gases. Triatomic gases have only a modestly greater molar specific heat at 2000K, e.g. 60for CO2 or 46atmosphere's ability to transport heat, is mostly determined by surface pressure and molecular weight. The mean molecular weight also affects the speed of gravity waves in the atmosphere, through its influence on the gas constant. This speed determines the character of many atmospheric waves which directly transport heat and are implicated in the generation of super-rotating low-latitude jets, which also transport heat. We present our simulation results in terms of a range of H2-N2 mixtures, but they would apply accurately to any other diatomic mixture with the same molecular weight, and with only moderate inaccuracy to triatomic-dominated mixtures.

Atmospheric Circulation

The measured phase curve of 55 Cnc e exhibits two features that demand substantial horizontal heat transport. First, the hot spot of the planet is shifted 41■ eastward relative to the substellar point. Second, the nightside temperature of the planet is quite high – on the order of 1300K – demanding delivery of 1.6 × 105W/m2 of heating to maintain it. However, the day-night temperature difference is also large – on the order of 1300K – which puts a limit on the efficiency of the heat transporting mechanism. It has been suggested that the implied heat transport on 55 Cnc e might be carried by the magma ocean. However, Kite et al. (2016) argued that a magma ocean could not redistribute enough heat to affect a planet's measured phase curve. It is also conceivable that tidal heating could contribute to maintaining the night-side temperature. In this paper, we will focus on the question of whether atmospheric heat transport alone can account for the phase curve, though we will offer some remarks in Section 5 on problems with tidal heating as an explanation of the night-side temperature. The hot-spot phase shift and phase curve amplitude on tide-locked planets have been extensively studied in connection with interpretation of Hot Jupiter phase curves. For sufficiently short period orbits, the global circulation of such atmospheres is dominated by the effects of planetary scale equatorial Rossby and Kelvin waves which drive a superrotating jet (Showman Polvani (2011), Heng Showman (2015)). The circulation system transports heat eastwards around the equator, shifting the hot-spot from the substellar point and warming the night-side of the planet. The observed phase curve of 55 Cnc e poses the particular challenge that its large 41■ hot-spot shift suggests strong heat redistribution, but its large 1300 K day-night difference suggests weak heat re-

distribution. The need to negotiate the tension between these two requirements puts strong constraints on the kind of atmosphere the planet can have.

7.2 Simulating a Lava Planet

7.3 Simplified Scaling Theory

Zhang

7.4 Idealised Simulations

7.4.1 Mean Molecular Weight

7.4.2 Surface Pressure

7.4.3 Optical Thickness

7.4.4 Vertical Structure

7.4.5 Phase Curves

7.5 Discussion

Chapter 8

Clouds on Lava Planets

> *"One face is forever sunlit, and one forever dark, and only the planet's slow liberation gives the twilight zone a semblance of seasons."*
>
> — Stanley G. Weinbaum, *The Lotus Eaters*

Cloud-covered exoplanets are a great problem for exoplanet observers, turning illuminating spectra into flat lines. Uniform cloud cover can be an issue, but heterogenous cloud cover may be useful.

Hot Jupiters are suggested to have cloud cover. Lava planets could have

In this chapter, I address the outstanding question from Chapter X – could the difference between our model results of 55 Cancri e and the observed low night-side temperature be due to high night-side clouds? I also discuss the effect of clouds on global circulation

and on observables such as hot-spot shift.

8.1 Clouds on Lava Planets

8.2 Simulations of Clouds

8.3 Effect on Observations

Chapter 9

Conclusions

Lorem ipsum dolor sit amet, consectetuer adipiscing elit. Ut purus elit, vestibulum ut, placerat ac, adipiscing vitae, felis. Curabitur dictum gravida mauris. Nam arcu libero, nonummy eget, consectetuer id, vulputate a, magna. Donec vehicula augue eu neque. Pellentesque habitant morbi tristique senectus et netus et malesuada fames ac turpis egestas. Mauris ut leo. Cras viverra metus rhoncus sem. Nulla et lectus vestibulum urna fringilla ultrices. Phasellus eu tellus sit amet tortor gravida placerat. Integer sapien est, iaculis in, pretium quis, viverra ac, nunc. Praesent eget sem vel leo ultrices bibendum. Aenean faucibus. Morbi dolor nulla, malesuada eu, pulvinar at, mollis ac, nulla. Curabitur auctor semper nulla. Donec varius orci eget risus. Duis nibh mi, congue eu, accumsan eleifend, sagittis quis, diam. Duis eget orci sit amet orci dignissim rutrum.

Nam dui ligula, fringilla a, euismod sodales, sollicitudin vel, wisi. Morbi auctor lorem non justo. Nam lacus libero, pretium at, lobortis vitae, ultricies et, tellus. Donec aliquet, tortor sed accumsan bibendum, erat ligula aliquet magna, vitae ornare odio metus a mi.

Morbi ac orci et nisl hendrerit mollis. Suspendisse ut massa. Cras nec ante. Pellentesque a nulla. Cum sociis natoque penatibus et magnis dis parturient montes, nascetur ridiculus mus. Aliquam tincidunt urna. Nulla ullamcorper vestibulum turpis. Pellentesque cursus luctus mauris.

Nulla malesuada porttitor diam. Donec felis erat, congue non, volutpat at, tincidunt tristique, libero. Vivamus viverra fermentum felis. Donec nonummy pellentesque ante. Phasellus adipiscing semper elit. Proin fermentum massa ac quam. Sed diam turpis, molestie vitae, placerat a, molestie nec, leo. Maecenas lacinia. Nam ipsum ligula, eleifend at, accumsan nec, suscipit a, ipsum. Morbi blandit ligula feugiat magna. Nunc eleifend consequat lorem. Sed lacinia nulla vitae enim. Pellentesque tincidunt purus vel magna. Integer non enim. Praesent euismod nunc eu purus. Donec bibendum quam in tellus. Nullam cursus pulvinar lectus. Donec et mi. Nam vulputate metus eu enim. Vestibulum pellentesque felis eu massa.

Quisque ullamcorper placerat ipsum. Cras nibh. Morbi vel justo vitae lacus tincidunt ultrices. Lorem ipsum dolor sit amet, consectetuer adipiscing elit. In hac habitasse platea dictumst. Integer tempus convallis augue. Etiam facilisis. Nunc elementum fermentum wisi. Aenean placerat. Ut imperdiet, enim sed gravida sollicitudin, felis odio placerat quam, ac pulvinar elit purus eget enim. Nunc vitae tortor. Proin tempus nibh sit amet nisl. Vivamus quis tortor vitae risus porta vehicula.

Bibliography

Demory, B.O. et al. Detection of a transit of the super-Earth 55Cancrie with warm Spitzer. *Astronomy & Astrophysics*, 533:A114, Sept. 2011.

Demory, B.O. et al. A map of the large day–night temperature gradient of a super-Earth exoplanet. *Nature*, 532(7598):207–209, Mar. 2016.

Heng, K. and Workman, J. Analytical models of exoplanetary atmospheres. I. Atmospheric dynamics via the shallow water system. *Astrophysical Journal, Supplement Series*, 213(2): 27, Aug. 2014.

Matsuno, T. Quasi-Geostrophic Motions in the Equatorial Area. *Journal of the Meteorological Society of Japan Ser II*, 44(1):25–43, 1966.

Pierrehumbert, R.T. and Hammond, M. Atmospheric circulation of tide-locked exoplanets. *Annual Reviews, Submitted*, 2018.

Showman, A.P. and Polvani, L.M. Equatorial Superrotation on Tidally Locked Exoplanets. *The Astrophysical Journal*, 738(1):71, Sept. 2011.

Vallis, G.K. Atmospheric and Oceanic Fluid Dynamics. *Atmospheric and Oceanic Fluid Dynamics*, pages 770–, Nov. 2006.

Winn, J.N. et al. A Super-Earth Transiting a Naked-Eye Star . *The Astrophysical Journal*, 737(1):L18, Aug. 2011.

Appendix A

Exo-FMS

The GCM Exo-FMS.

A.1 Model Structure

A.2 Sharing Exo-FMS

Appendix B

GFDL-SDC

The Spectral Dynamical Core.

Appendix C

Pseudo-Spectral Methods

A Pseudo-Spectral method.

C.1 Beta-Plane

C.2 Spherical Geometry